Testing Passive UHF Tag Performance Evolution

Daniel G. Kuester*†, *Student Member, IEEE*, David R. Novotny*, Jeffrey R. Guerrieri*,
Zoya Popović†, *Fellow, IEEE*

* U.S. Department of Commerce, National Institute of Standards and Technology, Boulder, CO, USA 80304
{daniel.kuester, david.novotny, jeffrey.guerrieri} at nist.gov
† University of Colorado, Department of Electrical, Computer, and Energy Engineering, Boulder, CO, USA 80309
{daniel.kuester, zoya.popovic} at colorado.edu

***Abstract*—Trends in tag development since the introduction of the ISO 18000-6C and EPC Global standards are investigated empirically with measurements of power harvesting and backscattering performance from 20 samples of passive tags across 860-960 MHz. The population spans ages of 0 to 6 years, 9 tag manufacturers, and 3 chip manufacturers. All tags were still in working condition, except two 5-year-old tags that no longer responded to interrogations and a 3-year-old tag with a degraded chip-to-antenna bond. Despite steadily improving chips, some older tags show performance comparable to new tags.**

I. Introduction

Continued developments in 860-960 MHz RFID tag chips are reducing the minimum operating power that passive transponder ("tag") chips must absorb from transceivers ("readers"). With this trend comes the expectation that newer tags are useful at greater range, with the side effect that their backscattered replies are becoming fainter [1]. If this trend continues, existing interference effects [2] will be made worse. These factors combined suggest that detecting tag backscatter will become a more significant limitation on RFID deployment reliability. Unfortunately, RF performance test standards for tags are still maturing, and do not yet exist for readers. As a result, data necessary to predict system reliability is scarce. Without standardized, repeatable tests, datasheet specifications from different manufacturers cannot be meaningfully compared. This may be of particular concern to parties with strict reliability requirements for tracking high-value inventories. These parties must undertake the effort and expense of device testing themselves or via a third party.

This is in contrast with communication signaling, which has been more extensively standardized for interoperability. Typical commercial systems comply with the EPC Global "UHF Class 1 Gen 2" and ISO 18000-6C standards, which outline the operation and parameters of the half-duplex protocol used for UHF RFID. In the forward link, a reader transmits a modulated carrier towards a tag field, which harvests the incident energy to supply power for communication and processing circuitry. Each tag responds by time-varying its antenna load impedance, encoding information in the backscattered carrier. This modulated backscattering implementation, known as load modulation, forms the return link. This type of scattering process had previously been applied to antenna measurements [3] and espionage [4].

Passive UHF tags have been commercially available for most of the past decade. We wished to investigate how their performance has evolved. The results are presented here as RF measurements of turn-on and backscattering for a broad variety of 20 tags marketed as conformant with EPC Global Class 1 Gen 2 and ISO 18000-6C standards. Samples were chosen arbitrarily from a collection of hundreds from various manufacturers that has been stored indoors since 2005. This information applies to evaluating deployments in which readers must interrogate tags of varying age, and investigating the benefits of adopting new tags. These goals require tests that give accurate indications of realistic signal levels in and out of the reader, and give results which can be used to accurately compare performance between different tags.

Power harvesting and scattering performance measurements are described in current test standards, but they are still maturing and have unresolved sources of uncertainty. Instead, we present measurements of transmit and backscattered power calibrated to a common microwave network interface. The results have high relative accuracy for comparing the tags (limited by the testbed measurement linearity and positioning error of the samples in the test environment), but lack the more general predictive uses of full black box characterizations.

II. Backscatter measurement method

A. Existing Test Standards

Results from tests that comply with existing standards have the advantage of implicitly conveying measurement details, as well as a sense of the accuracy of the measurements. If the standards give methods that achieve low measurement uncertainty, careful testing between different labs can validate conclusions by repeating the same tests in their own facilities. This section will outline why the authors concluded that the test methods in existing standards are not yet repeatable enough for use in this paper.

Performance test standard ISO/IEC 18046-3 [6] outlines a general test for the threshold field strength necessary to activate a tag, but offers no specific approach for determining field strength. Tag scattering, which is becoming a more significant system range constraint as tags improve [1] and especially when interference is present [2], is addressed only in protocol conformance test standards.

The 2006 version of standard ISO 18047-6 [7] prescribes a tag backscattering conformance test characterized as the

difference between the radar cross section values between the tag's two load modulation states. The test method calibrates measurements of tag backscattering against the change in received power caused by adding a thin rod to the test environment. Adding and removing the entire thin rod calibration standard introduces systemic error by modulating the structural-mode scattering from the rod, which interacts with multipath in the test environment differently [1] from tags' antenna-mode [8][9] scattering. The use of such an electrically small calibration target requires faith in the accuracy of the analysis used to compute its radar cross-section (RCS), which makes the measurement result untraceable to fundamental physical standards of any national metrology laboratory. These errors may make measurement results challenging to repeat between different testbeds, and as a result some parties may choose not to undertake the expense of running the tests. This approach can introduce significant systemic error by neglecting phase, though many existing papers have discussed how phase can be included, e.g. [8][9][10].

The 2011 version of the ISO 18047-6 conformance test standard computes "Delta RCS" for a device-under-test by inserting measurements of range and antenna gain parameters into the radar equation, and incorporates phase measurements. The uncertainty of results from this approach has been estimated at approximately 2 dB in a paper that used a similar approach [11]. With spectrum analyzer backscatter measurements, however, drift and automatic realignments corrupt the relative accuracy of measurements of tags taken at different times.

While calibration errors may not introduce problems in comparing tag performance, they will introduce errors in measurements of the absolute signal levels in and out of a reader. To avoid this problem, at the sacrifice of the generality offered by a "black box" tag characterization, results in this paper are from measurements of available power transmitted into and received from the test antennas. Transmitted power is measured with a directional coupler and power sensor, and backscattered power is measured with the calibration introduced in [5].

B. General Testbed Configuration

The hardware and performance cababilities of the testbed are summarized in Fig. 1 and Table I. In this approach, reference modulation, which is backscattered from the antenna shown on the right, is used to calibrate backscatter measurements from each sample. The details of the method can be found in [5].

The available power for interrogation out of the power amplifier is computed from S-parameter measurements of the coupler and the transmit and receive antennas. The interrogator and power amplifier feed a transfer switch, which allows either antenna to be the transmit or receive antenna. Measurements of output signal levels coupled into the spectrum analyzer showed linearity errors below 0.1 dB up to 32 dBm output.

The testbed antennas shown in Fig. 1 are encapsulated in the network S. They are two different models of commercially available linear-polarized patch antennas with nominal boresight gains of 8 dBi. They have return losses above 12 dB across 860-960 MHz.

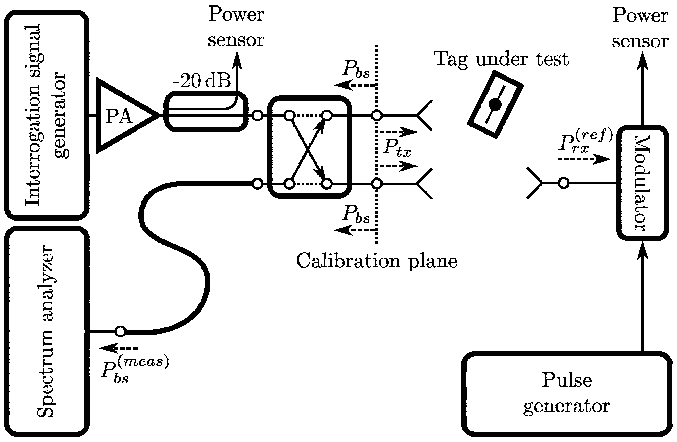

Fig. 1. Tag backscattering testbed. P_{tx} corresponds to transmit power available to the input of S, and P_{bs} is the backscattered power out of the non-transmit port of S that is available to the receiver. Reference backscatter, generated on the right, is used to calibrate measurements of tag backscatter as in [5].

TABLE I
TESTBED SPECIFICATIONS ACROSS 860-960 MHZ

Testbed antennas	Horizontally polarized patches
Transmit power resolution	0.1 dB
Nominal antenna gains (boresight)	8 dBi
Antenna to antenna isolation	>45 dB
Transmit power	<35 dBm
Interrogator return loss	>20 dB
Measurement noise	<-135 dBm/Hz

The antenna used to generate reference modulation is a pyramidal horn with 6 dBi nominal gain, oriented toward the testbed antennas to maximize the strength of the reference signal. The modulated power received from the reference antenna in this configuration is between -60 dBm and -20 dBm. The application of the reference signal to tag backscatter calibrations are summarized in Section II-D.

These antennas, as well as the DUT, are co-polarized and in a semi-anechoic environment described in Fig. 2. Each DUT is mounted in the position shown, on a dielectric chosen to approximately match the design purpose suggested in the manufacturers' specifications.

The reference and DUT backscatter signals are measured with a spectrum analyzer, controlled externally with software through GPIB. Modulation measurement and analysis with these tools are described in the next section.

C. Transmit Power Measurements

The testbed introduced in the previous section uses a 20 dB directional coupler to determine available power into the testbed's transmit antenna. Measurements of the minimum transmit power level necessary to turn on various tags serve as comparative measures of tags' power harvesting performance. Turn-on power measurements are also necessary for

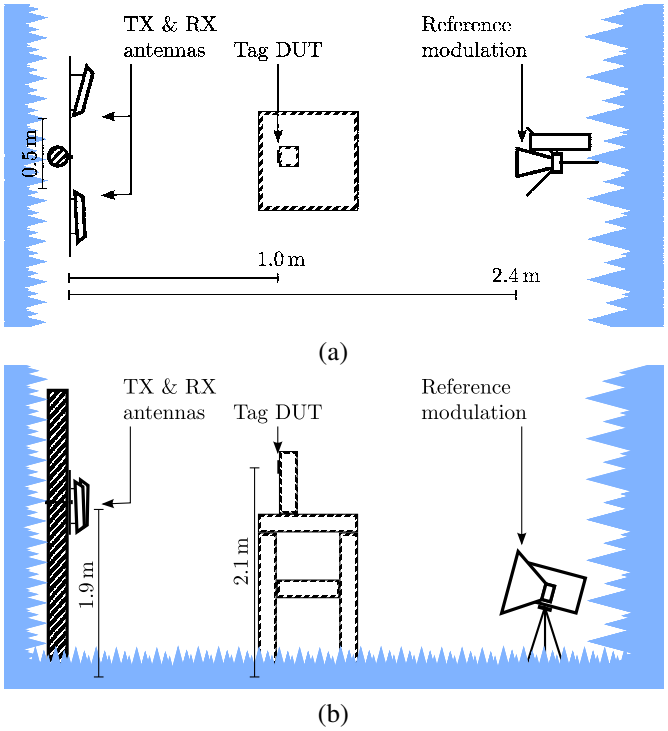

Fig. 2. Antenna arrangement in the test zone shown (a) from the top and (b) from the side. The reference modulation target is below the DUT to maintain adequate dynamic range by minimizing shadowing.

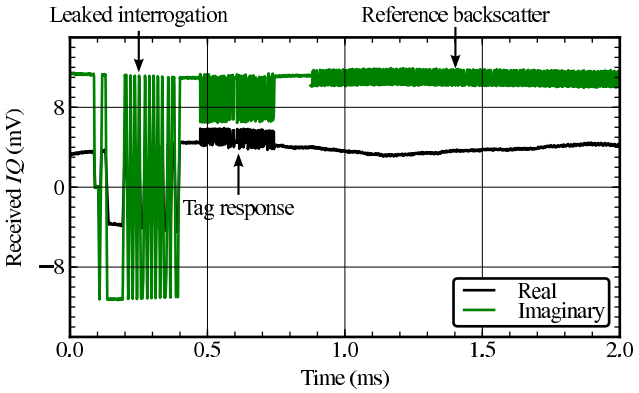

Fig. 3. A demodulated trace from a transaction at 910 MHz with an ISO/IEC 18000-6C tag received by a spectrum analyzer. It shows leaked interrogation modulation from the forward link, the tag response from the reverse link, and reference backscatter from the calibration device introduced in this paper. In use, the reference backscatter is only enabled during measurement to avoid interfering with the tag.

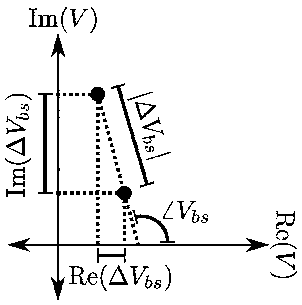

Fig. 4. Illustration of demodulated ΔV_{bs} on the complex (IQ) plane received from a reference backscatterer. The signal is shown in rectangular coordinates as $\mathrm{Re}(\Delta V_{bs}) + j\mathrm{Im}(\Delta V_{bs})$, and in polar form as magnitude and phase.

tag backscatter calibrations, which will be discussed in the next subsections.

S-parameter measurements of the directional coupler integrated with the transfer switch, which feed S, were performed with a network analyzer. The network consists of 3 ports: input (port 1), output to the antennas (port 2), and coupling into the power sensor (port 3). Measurements of the reflection coefficients of the two testbed patch antennas were performed as well, each with different Γ_{ant}. The generator output was padded with a circulator and attenuator with reflection coefficient Γ_G. We assume high coupler directivity so that $S_{23} = S_{32} = 0$ to simplify analysis, and that the power sensor is well-matched to the coupled port. The finite 40 dB directivity specified for our coupler and coupling factor errors introduce an uncertainty of approximately 0.1 dB to power measurements.

Under these conditions, the wave magnitude $|a_1|$ into the coupler, input measured power at the coupler $P_{tx}^{(meas)}$, and coupler output wave magnitude $|b_2|$ are related by [12]

$$\frac{P_{tx}^{(meas)}}{|a_1|^2} = \frac{|S_{31}|^2}{|1-\Gamma_{in,1}\Gamma_G|^2}, \tag{1}$$

where $\Gamma_{in,1}$ is the reflection coefficient looking into the input of the loaded coupler given by

$$\Gamma_{in,1} = S_{11} + \frac{S_{21}S_{12}\Gamma_{ant}}{1-S_{22}\Gamma_{ant}} \tag{2}$$

and

$$\frac{|b_2|^2}{|a_1|^2} = |S_{21}|^2. \tag{3}$$

Combining and solving for $|b_2|$ gives

$$|b_2|^2 = P_{tx}^{(meas)} \frac{|S_{31}|^2}{|S_{21}|^2|1-\Gamma_{in,1}\Gamma_G|^2}. \tag{4}$$

In this paper, reported transmit power levels P_{tx} are available power quantities computed as

$$P_{tx} = \frac{|b_2|^2}{1-|\Gamma_G|^2}. \tag{5}$$

Threshold transmit power P_{tx0} is simply the available transmit power evaluated at the minimum level necessary to turn on a tag.

D. Backscattered Power Measurements

Backscattered power $P_{bs}^{(tag,meas)}$ and $P_{bs}^{(ref,meas)}$ are measured with *IQ* demodulation on a spectrum analyzer. Example signal traces are shown in Fig. 3. The interrogation signal is an ISO/IEC 18000-6C query command, with tag and reference responses modulated at 160 kHz.

Tag backscatter and reference modulation are measured over periods of 240 µs and 1 ms, respectively. Connecting the 10 MHz frequency reference from the spectrum analyzer to the RFID interrogation source, carrier phase noise was less than $1.3°$ per symbol at 160 kHz modulation, introducing negligible error to measurements of signal levels between adjacent symbols. Across entire tag or reference signal traces, however, the carrier drifts by up to $13°$. This made separating the signal into the two states in software ("clustering") more challenging: slow drift in each of the I and Q components was often larger than the backscattered signal, making the straightforward histogram analysis suggested by IEEE 181 [13] unsuitable.

Instead, states are clustered by applying a Gaussian filter to the I and Q scattering components, and finding sharp peaks after differentiating the result. These peaks are detected by searching for local amplitude maxima above a threshold set (somewhat arbitrarily) to the standard deviation of the filtered signal. The Gaussian filter is useful here because it removes noise without shifting pulse edges. This is a simpler one-dimensional implementation of Canny edge detection [14].

The values of V_I and V_Q in each cluster are then computed, reducing noise. Their differences, ΔV_I and ΔV_Q, form orthogonal components of the complex backscattered signal phasor ΔV_{bs},

$$\Delta V_{bs} = (\Delta V_I + j\Delta V_Q) \exp j\phi, \tag{6}$$

where ϕ is the arbitrary phase reference of the I-Q plane. A geometric interpretation of ΔV_{bs} with the two modulation states is illustrated in Fig. 4. This quantity is measured for each signal transition in a transaction measurement. For work presented here, the 60-80 pulse transitions were measured and averaged for 8 transactions, which resulted in a measurement noise floor below than -95 dBm.

The measured power in these two states is calculated as [8][10][15][16].

$$P_{bs}^{(meas)} = \frac{|\Delta V_{bs}|^2}{2Z_0} = \frac{|\Delta V_I + j\Delta V_Q|^2}{2Z_0}. \tag{7}$$

The more accurate calibrated power P_{bs} is then computed as the final result, with the method described in [5].

Measurements of tag backscatter and reference backscatter on the right side of Fig. 1 are computed this way. Comparing the backscattered power measurement with the value predicted by the model of [5] allows linear measurement losses from cable losses, instrument misalignment, and mismatch to be computed. Removing this loss from the tag measurement gives the final calibrated result.

III. Sample Tag Measurements

Samples of twenty different passive EPC Class 1 Gen 2 inlays were selected arbitrarily for testing. They represent 9 different inlay manufacturers, and at least 6 different tag chip products from 3 different chip manufacturers. The tags' ages vary from 0 to 6 years. The distribution of these parameters, as well as the printed antenna surface area of each inlay, are outlined in Table II. The trade names of the manufacturers and products are not disclosed, because of restrictions in the authors' institution, and because the tests may not have been performed with each tag tuned precisely on an the intended dielectric for a fair comparison.

TABLE II
Tag Sample Distribution

Tag	Inlay Make	Inlay size (cm^2)	Chip	Age (years)
1	1	11	A	3
2*	2	12	B	6
3‡	3	6.8	A	1
4*‡	3	2.0	A	2
5	3	63	C	5
6	4	12	A	3
7	5	29		4
8	6	88		3
9†	4	10	A	3
10	7	12		4
11	8	48	D	4
12	3	19	A	5
13*	9	46		5
14	9	6.0		5
15*†	9	37		5
16	6	92		5
17	3	23	E	0
18	3	11	F	1
19	3	12	A	1
20	3	53	E	1

* No response up to 33 dBm transmit power
† Distorted backscatter waveform
‡ Tuned for operation on plastic or glass

TABLE III
EPC Global & ISO/IEC 18000-6C tag query parameters

Reader-to-tag modulation	PR-ASK
Tag-to-reader modulation	FM0
Tag-to-reader link rate (BLF)	160 kHz
Reader-to-tag link rate	160 kHz (data 0)
	91 kHz (data 1)
Anticollision slots (Q)	0 (no slots)
Delay after tag response† (T2)	1 ms
Tari	6.25 µs

The tags are grouped into three broad categories related to their size and antenna properties. "Small" tags (with area less than 10 cm^2) are based on dipoles, but with large bends to raise the input impedance for better chip matching. Many of these tags were also designed for operation on dielectric materials; these tags were mounted on plexiglass. "Medium" sized tags (10 cm^2 to 25 cm^2) are similar to half-wavelength dipoles, but with smaller bends that match to the tag chip while maintaining a more linear polarization. Most "large" (more than 25 cm^2) tag antennas were effectively two "medium" antennas oriented orthogonally for dual polarization. During tests, tag antennas were oriented as nearly co-polarized with the testbed's transmit and receive antennas as possible. The gain and propagation losses in this configuration were expected to be similar among single-polarized medium and large tags, and approximately 3 dB smaller for dual-polarized tags.

Tags were interrogated with the protocol parameters listed in Table III. The tag backscatter measurement is meaningful only with enough power to turn on, so measurements at each frequency are reported only at or above the minimum turn-on

power for the tag. In linearity tests, power levels are reported as relative to this power level, in part to fit different results on the same axes.

Several of the tags were marked in Table II as exhibiting "no response" or "distorted backscatter," anywhere across 860-960 MHz in the position pictured in Fig. 2 up to 33 dBm transmitter power. Additional tests of tags 2 and 15 closer to the testbed antenna still result in no response. Tags 4 and 13, however, did respond to the stronger field closer to the antenna; a different dielectric may have resulted in a better chip-antenna match in the tag and a measureable response at 1 m. The response from Tag 9 was inconsistent and did not exhibit clear discrete scattering states. On close examination of the tag (and other samples of the same model) the authors observed brown discoloration at the chip-to-antenna bond, and believe it may have degraded.

A. Turn-on Power Measurements

Swept-frequency measurements of the minimum available power P_{tx0} into each transmit antenna needed to turn on each tag is plotted in Fig. 5. Tests were performed with each antenna as a transmitter and receiver by repeating the tests after toggling the transfer switch. Tags are grouped by size and colored to suggest their approximate age. Smaller values of P_{tx0} indicate a reduced turn-on requirement, and improved tag performance in this measurement configuration. Across 902-928 MHz, the newest tag needed the least power to turn on, but near 868 MHz, a 4-year-old tag performed best.

In general, while in many cases newer tags performed better, this was not universally the case. While not visible on the plots, tags designed for operation on dielectrics exhibited the strongest frequency dependences. Among all of the tags at any given frequency point, there was variation of up to 25 dB between the largest and smallest turn-on power. There was also no significant performance difference between the co-polarized medium tags and the dual-polarized large tags.

B. Backscattering Measurements

Backscattered power from each tag was measured with frequency and power sweeps and into each antenna by use of the transfer switch. Swept-frequency measurements (Fig. 6) were performed at 0.8 dB above the turn-on threshold, like the "ΔRCS" tests in ISO/IEC 18047-6. The power sweeps (Fig. 7) were performed at 910 MHz, the middle of the global 860-960 MHz band and inside the U.S. 902-928 MHz band.

Higher backscattered power corresponds to a stronger signal that is more easily detected by a reader. As predicted in [1], backscatter received from newer tags is actually weaker: when newer chips can operate with less power than older ones, less incident power is available for backscattering to the reader. Even if all tags were excited with the same power level, newer tags would still return less power; because of their reduced turn-on threshold, newer tags would opererate at a higher compression point, causing compression in the backscattered signal [17].

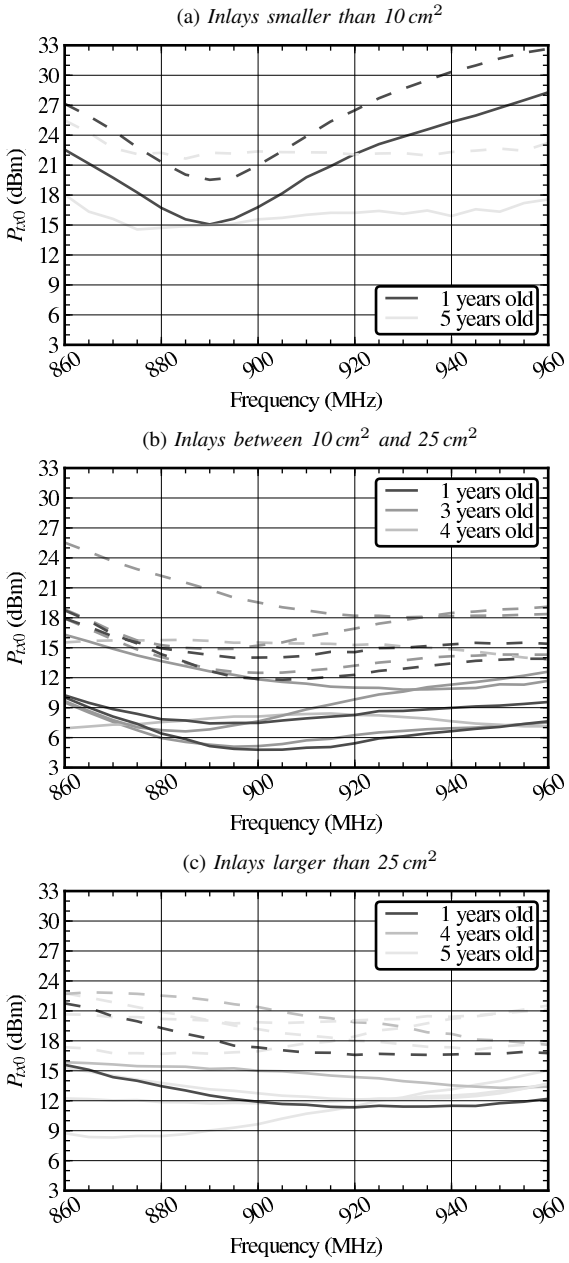

Fig. 5. Minimum power transmit into reader antenna for tag turn-on. Solid lines and dashed lines correspond to transmission from the antenna shown at the top and bottom of Fig. 1(a), respectively.

We also examine the power backscattered from a tag as the transmit power is raised above the minimum turn-on level in Fig. 7. The backscattered response linearity varied among the various tags: 20 dB above the transmit turn-on power, some tags responded with nearly the same backscattered power as at turn-on, while others' responses were 10 dB stronger.

C. Uncertainty

Uncertainty estimates of the measured results are summarized in Table IV. Backscattered power measurement uncertainty is discussed in more detail in [5].

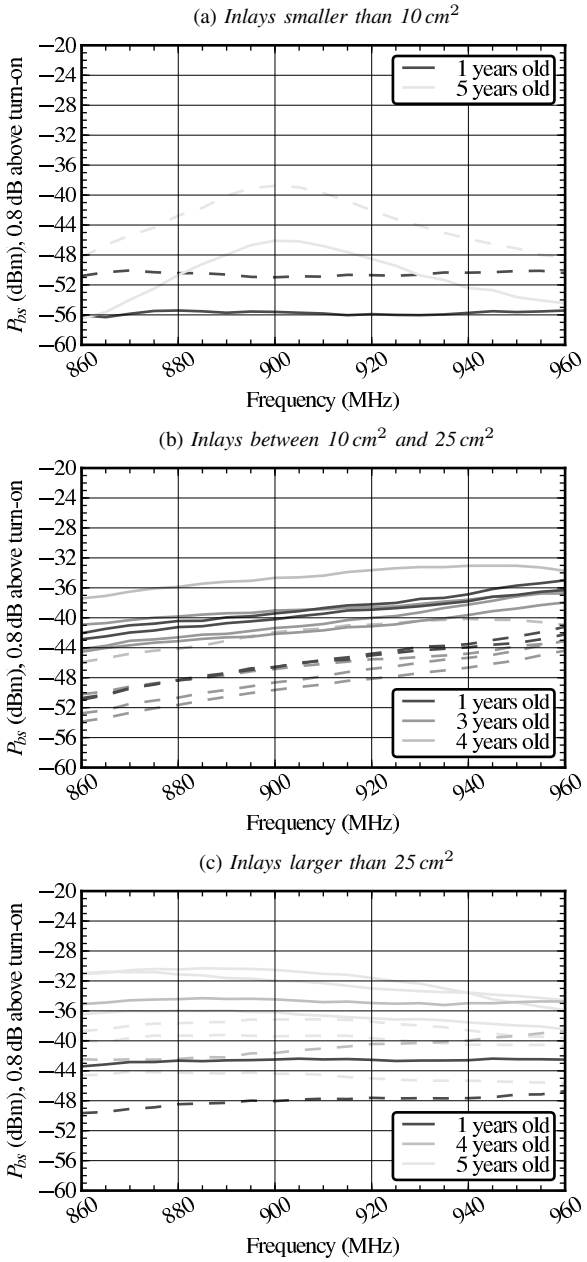

Fig. 6. Measurements of received backscattered power from tags at 0.8 dB above each tag's turn-on sensitivity threshold plotted against frequency. Solid lines and dashed lines correspond to transmission from the antenna shown at the top and bottom of Fig. 1(a), respectively.

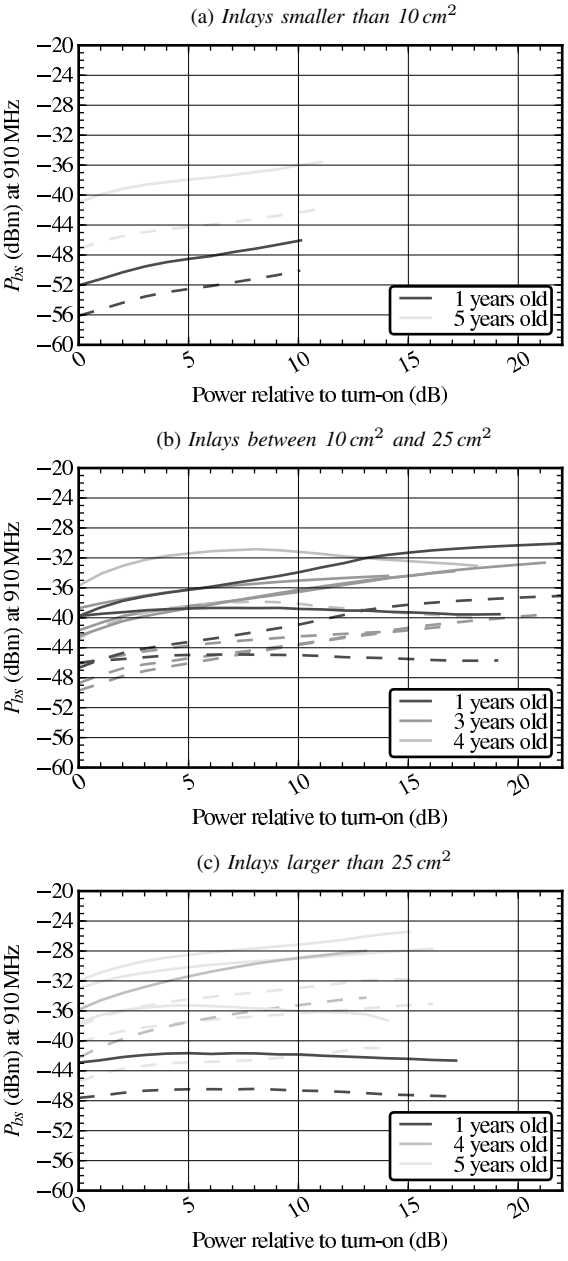

Fig. 7. Measurements of received backscattered power from tags at 910 MHz, plotted against power normalized to each tag's turn-on threshold. Power levels were swept from from the tag turn-on level (0 dB on the plot) to the maximum supported by the testbed. Solid lines and dashed lines correspond to transmission from the antenna shown at the top and bottom of Fig. 1(a), respectively.

Turn-on transmit power (P_{tx0}) uncertainty is estimated according to documentation by the power meter and power sensor manufacturer, documentation and a set of verification standards from the network analyzer manufacturer, and tests of tag turn-on level repeatability. The tag turn-on level is the largest single source of uncertainty in the transmit power measurement.

IV. Conclusion

Though tags less than one year old were among the easiest to turn on, several products up to four years old were still competitive. Some older tags did not respond at all, however, and may have degraded with age. This sample size is too limited for a specific recommendation, but periodic checks for dead tags may be beneficial as deployments age.

As expected, we measured weaker backscatter from newer

TABLE IV
EXPANDED UNCERTAINTY ESTIMATES (COVERAGE FACTOR 2)

(a)

DUT backscattered power, P_{bs}	
M calibration	± 0.25 dB
Power meter and sensors	± 0.25 dB
Multiple reflections	± 0.15 dB
IQ level measurements	± 0.05 dB
Noise and nonlinearity	± 0.1 dB
Expanded uncertainty	± 0.4 dB

(b)

DUT threshold power, P_{tx0}	
Turn-on threshold repeatability	± 0.2 dB
Power meter and sensor	± 0.15 dB
Coupling errors	± 0.1 dB
Noise and nonlinearity	± 0.1 dB
Turn-on threshold resolution	± 0.05 dB
Expanded uncertainty	± 0.3 dB

tags. The backscattered signal was above the sensitivity manufacturers specify for typical readers, but the weaker signal makes interference from other transmitters a greater threat to system operation. Future work may need to investigate the threat this poses to communication reliability between readers and tags.

Tags uniformly used newer chips that require less power to activate, but correlation between tag age and performance was weak. A possible explanation is that antenna-to-chip mismatch losses change significantly between tag models, in part because some were optimized for mounting on particular dielectrics instead of in free space. This underscores the importance of tag impedance tuning, which appears to have a more significant impact on system behavior than incremental tag chip improvements.

This significance suggests that tag matching effects may be a useful area for further development in theory and testing standards. While detuning effects play a significant role in realistic system behavior, turn-on performance and scattering characterizations are defined in free space. Prescribed test methods for a tag's turn-on field strength or modulated RCS assume ideal free space behavior, which does not apply in the presence of detuning objects. Further developments that define tag tests and characterizations in realistic environments may enable improved link analysis and design to help optimize performance in real deployments.

V. ACKNOWLEDGEMENTS

Z. Popovic acknowledges support from the Hudson Moore Jr. professorship at the University of Colorado.

The United States Department of Homeland Security Science and Technology Directorate has, in part, sponsored the production of this material with NIST, under contract HSHQDC-09-X-00305.

REFERENCES

[1] D. G. Kuester, D. R. Novotny, and J. R. Guerrieri, "Forward and Reverse Link Constraints in UHF RFID with Passive Tags," in *Proceedings of the 2010 IEEE Symposium on Electromagnetic Compatibility*, 2010, pp. 680–685.

[2] M. Souryal, D. Novotny, D. Kuester, and J. Guerrieri, "Impact of RF Interference between a Passive RFID System and a Frequency Hopping Communications System in the 900\,MHz ISM Band," in *Proceedings of the 2010 IEEE Symposium on Electromagnetic Compatibility*, 2010, pp. 495–501.

[3] J. Richmond, "A modulated scattering technique for measurement of field distributions," *Microwave Theory and Techniques, IRE Transactions on*, vol. 3, no. 4, pp. 13–15, 1955.

[4] A. Glinsky, *Theremin: Ether Music and Espionage*. Champaign, IL, USA: University of Illinois Press, 2000.

[5] D. Kuester, D. Novotny, J. Guerrieri, R. Direen, and Z. Popovic, "Reference Modulation for Calibrated Measurements of Tag Backscatter," in *Proceedings of the IEEE Conference on RFID*, 2011, p. submitted for publication.

[6] "ISO/IEC 18046-3: Radio frequency identification device performance test methods — Test methods for tag performance," Tech. Rep., 2007.

[7] "Radio frequency identification device conformance test methods — Test methods for air interface communications at 860\,MHz to 960\,MHz," ISO/IEC standard 18047-6, Tech. Rep., 2006.

[8] P. Nikitin and K. Rao, "Theory and measurement of backscattering from RFID tags," *IEEE Antennas and Propagation Magazine*, vol. 48, no. 6, pp. 212–218, 2006.

[9] J. Bolomey, S. Capdevila, L. Jofre, and J. Romeu, "Electromagnetic Modeling of RFID-Modulated Scattering Mechanism. Application to Tag Performance Evaluation," *Proceedings of the IEEE*, vol. 98, no. 9, pp. 1555–1569, 2010.

[10] S. Skali, C. Chantepy, and S. Tedjini, "On the measurement of the delta Radar Cross Section (ΔRCS) for UHF tags," in *2009 IEEE International Conference on RFID*. IEEE, Apr. 2009, pp. 346–351.

[11] A. Pouzin, T. P. Vuong, S. Tedjini, M. Pouyet, J. Perdereau, and L. Dreux, "Determination of measurement uncertainties applied to the RCS and the differential RCS of UHF passive RFID tags," in *Antennas and Propagation Society International Symposium, 2009. APSURSI '09. IEEE*, 2009, pp. 1–4.

[12] D. Kerns and R. Beatty, *Basic Theory of Waveguide Junctions and Introductory Microwave Network Analysis*. Oxford: Pergamon Press, 1967.

[13] "IEEE Std 181-2003: Standard on Transitions, Pulses, and Related Waveforms," Institute of Electrical and Electronics Engineers, Tech. Rep., 2003.

[14] J. Canny, "A Computational Approach to Edge Detection," *IEEE Transactions on Pattern Analysis and Machine Intelligence*, vol. PAMI-8, no. 6, pp. 679–698, Nov. 1986.

[15] F. Fuschini, C. Piersanti, F. Paolazzi, and G. Falciasecca, "Analytical Approach to the Backscattering from UHF RFID Transponder," *Antennas and Wireless Propagation Letters, IEEE*, vol. 7, pp. 33–35, 2008.

[16] A. Pouzin, T. P. Vuong, S. Tedjini, M. Pouyet, and J. Perdereau, "Bench test for measurement of differential RCS of UHF RFID tags," *Electronics Letters*, vol. 46, no. 8, pp. 590–592, Apr. 2010.

[17] L. Mayer and A. Scholtz, "Sensitivity and impedance measurements on UHF RFID transponder chips," in *Int EURASIP Workshop on RFID Techn., Vienna, Austria*, 2007, pp. 1–10.